PAN

Opto-Electronics Review

journal homepage: https://journals.pan.pl/opelre

Investigation of transmission properties of a tapered optical fibre with gold nanoparticles liquid crystal composite cladding

Joanna E. Moś*, Karol A. Stasiewicz, Leszek R. Jaroszewicz

Faculty of New Technologies and Chemistry, Military University of Technology, 2 Kaliskiego St., 00-908 Warsaw, Poland

Article info

Article history:
Received 23 Aug. 2022
Received in revised form 11 Oct. 2022
Accepted 13 Oct. 2022
Available on-line 23 Nov. 2022

Keywords:
Tapered optical fibre; liquid crystals; liquid crystal composites; nanoparticles; optical sensor.

Abstract

The article presents a study of a hybrid structure based on the combination of a tapered optical fibre and gold nanoparticles dispersed in a liquid crystal material. Sensitivity to changes of the refractive index of the environment in which the structure is located, as well as the possibility of changing the refractive index of liquid crystals by external factors, such as temperature and electric field, were investigated. Electro- and thermally-induced changes of the refractive index of a liquid crystal through the rotation of a molecule director, which cause changes in the light propagated in a tapered optical fibre, were described. The most important issue in the article is to determine the influence of doping a liquid crystal with gold nanoparticles the concentration of which varies between 0.1 and 0.3 wt.%. The paper presents transmission measurements in a wide optical range depending on voltage, temperature, and frequency changes. Additionally, time courses of the obtained signal were measured. The study shows that the appropriate selection of nanoparticle concentration has a huge impact on the optical wave propagation. The experimental results show that the optical changes obtained for the investigated hybrid structure prefer it for use as an electro-optical switcher, filter, or sensor.

1. Introduction

Much of the research is related to controlling a light beam, both in free space and various materials. Appropriate research and analysis of the information carried by the light beam allow getting knowledge about the world and ensure the development of new technologies in many areas of life [1–4]. The article describes research on an important part of this topic – optical fibres. This is due to the ability to control the properties of the propagating light in a hybrid combination of a tapered optical fibre (TOF) and a functional material [5–7]. Research on this type of connection has been intensively developed for many years. Currently, in the literature, it is possible to find information on the use of TOF of any diameter made of various types of fibres, including single-mode fibre (SMF), multi-mode fibre (MMF), photonic crystal fibre (PCF), and polymer optical fibre (POF), not only as a transmission medium but also as a sensor. There are many functional solutions using tapers in various configurations, such as biconical TOF [8, 9], fibre Bragg grating (FBG) [10, 11], long-period grating (LPG) [12, 13], Michelson [14] and Mach-Zehnder [15] interferometers, loop interferometer [16], coupler [17], as well as resonators (including multi loops, knots) [18, 19]. Hybrid combinations of various TOF configurations with a functional material have found application in many opto-electronic devices such as sensors, filters, and amplifiers. This is due to the possibility of improving the parameters of a given device through a conscious use of the properties of the functional material. It should be emphasized here that the choice of material to connect with the taper is huge. As a result, the possibility of conducting research work on this type of connection has great potential. The functional materials used, described in the literature, range from quantum dots [5, 20], through metals [21, 22], polymers [23, 24], oxides [25], graphene layers [26, 27], up to liquid crystals (LCs) [28–30]. To obtain an excellent sensor, the selected material should provide low optical loss for a specific wavelength range, effectively influence changes in the properties of the light beam guided through the fibre by an appropriate modification of material properties, and provide a quick response to changes in the tested parameter.

*Corresponding author at: joanna.mos@wat.edu.pl

https://doi.org/10.24425/opelre.2022.143936
1896-3757/ Association of Polish Electrical Engineers (SEP) and Polish Academic of Sciences (PAS). Published by PAS

Additionally, it should have a simple technology for bonding with glass and be inexpensive for practical applications [3, 31, 32]. TOF-based devices can operate based on various physical phenomena, such as absorption [33, 34], fluorescence [35], surface plasmon resonance (SPR) [36], and lossy mode resonance (LMR) [37].

This article describes the research on a hybrid combination of biconical TOF with LC doped with gold nanoparticles (Au:NPs). LCs are attractive materials that are widely used in optoelectronic applications. This is due to their anisotropic controllable properties via an external field or temperature [38]. The connection of TOF with LC allows to build an optoelectronic device, the basis of which is the tunable LC environment of TOF. The article describes the technology of TOF with pure LC material (as references) and LC doped with Au:NPs as gold nanoparticles liquid crystal composite (NPsLCC). The paper provides information on the effect of LC Au:NPs addition on changes in transmission properties under the influence of voltage and temperature. From theoretical analysis, it is known that NPs doping of LC affects physicochemical properties of LC materials. In the presented research, it is tested whether it also has a direct impact on changes in the properties of light propagating in the TOF.

2. Materials and methods

2.1. *Principle of TOF and gold nanoparticles liquid crystal composite combination*

Description of the light propagation in an optical fiber is widely presented in literature [5–7]. The most interesting description uses the Maxwell's equation to show the electromagnetic field propagating at the boundary of two materials with different refractive indices. It should be noticed that this description is focused mostly on light propagation in a core [24]. However, it should be taken into account that a part of the wave guided in the core penetrates the cladding as the evanescent field, which is described by the light beam parameter– penetration depth (d_p) (Fig. 1) [39]. This parameter depends on the wavelength used, refractive index of the fibre, and diameter of the core. Using the SMF, it is known that physically the cladding is a layer thick enough (for SMF≈125 μm) to isolate the light beam from the environment, and, in this case, the light beam guided in this structure cannot be affected by external factors.

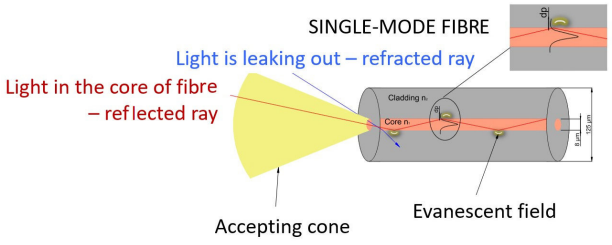

Fig. 1. Light guiding mechanism in the optical fibres (penetration depth).

Generally, TOF is produced by heating a section of fibre and tapering its standard size (Fig. 2). As a result, more wave enters the cladding (increases d_p) until the light

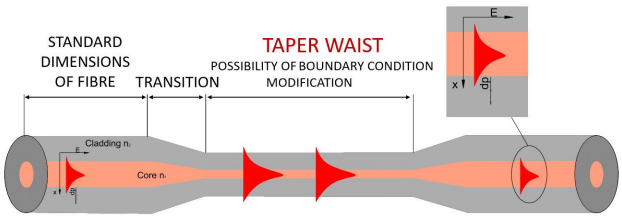

Fig. 2. Areas of a tapered optical fibre (TOF).

propagates through the entire taper waist. Thus, the mode field is expanded while the geometrical conditions of the TOF are limited [40]. It is because of this that a new structure obtained allows modifying the propagation conditions of the light beam by changing the boundary conditions – changing the refractive index (RI) of the TOF environment. The use of additional material in the TOF area, and the conscious use of its properties, in particular, changes in material and optical parameters depending on an external factor, such as temperature, allows for controlling the properties of light propagating in TOF. Thus, using the anisotropic properties of the LC, it is possible to tune the RI value which detects TOF using an electric or magnetic field and temperature changes [28, 29].

The presented research is focused on a combination of the optical fibre element (TOF) and the LC as a material which RI can be controlled by the electric field and temperature. There are many articles in the literature describing the research on the optical properties of LC dopped with NPs. Most articles are connected with LCs combined with a variety of metal and oxide nanoparticles [41–45]. In the literature, Au:NPs are one of the most commonly used materials for LC composites [46, 47]. Doping changes dielectric anisotropy, elasticity constants, and rotational viscosity. Such changes improve all parameters of the created hybrid structure, including switching time, threshold voltage, temperature phase transition, and threshold voltage for the Fredericks transition [38, 48].

The basic phenomenon connected with the use of LC is that the refractive index with which the light interacts in the TOF structure is the average RI between n_e and n_o LC resulting from the alignment and change of orientation of the LC director around the TOF. Changes in this coefficient have a direct impact on the light transmission through TOF because this parameter is the basis for the light propagation conditions in the optical element under study.

2.2. *The technology of hybrid structure of TOF and liquid crystal with gold nanoparticles*

TOFs elements used as the base element in connection with LC were made on the arrangements named fibre optic taper element technology (FOTET) previously described in Refs. 7 and 29. A standard telecommunication SMF was used given its low cost. During the first technological stage, it is important to select an appropriate TOF for a given application with the selected material. A TOF with a too small diameter with a higher RI of the surrounding material may cause a total light leakage outside the TOF structure. On the other hand, a too large TOF diameter will not cause the expected transmission changes, and results in the use of much higher controlling factors such as electric field or

temperature, simultaneously increasing the response time. The TOF used in this article was characterized by an elongation of 19.94 ± 0.19 mm, a taper waist diameter of 14.5 ± 0.5 µm, and losses below 0.25 dB at 1550 nm. The movement of the FOTET torch was 5 mm which ensured the production of a long taper waist. Such TOF gives the possibility of interaction of the evanescence wave with the external material and makes it possible to control it. Moreover, at the FOTET, TOF was mechanically secured by building a special LC cell which was then filled with a selected LC mixture using capillary forces [Figs. 3(a) and 3(b)].

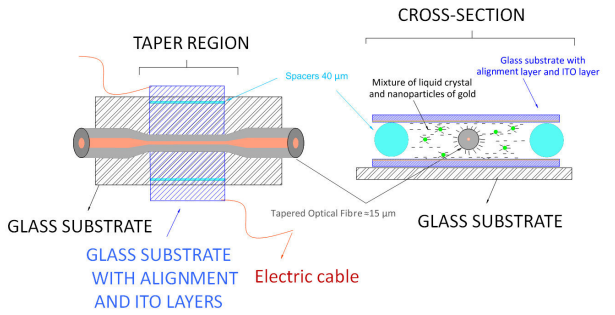

(a)

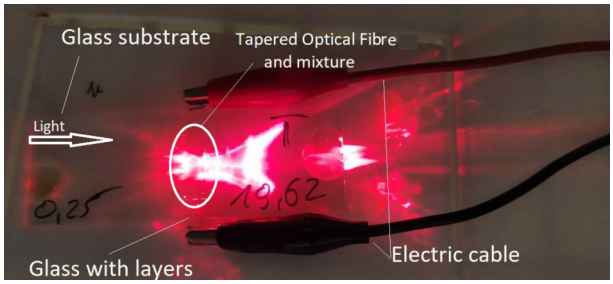

(b)

Fig. 3. Cell with a TOF and a liquid crystal with gold nanoparticles composite.

The cell consisted of two glasses with an LC orientation layer, about 5 mm wide (so that the 5 mm taper waist area was surrounded by LC) and a conductive layer – indium tin oxide (ITO). The application of LC orientation layers allowed to produce cells characterized by perpendicular (⊥), parallel (∥), or twisted (T) orientation in correlation with the TOF axis (Fig. 4). The orientation of the cell gives the initial alignment of the LC molecules.

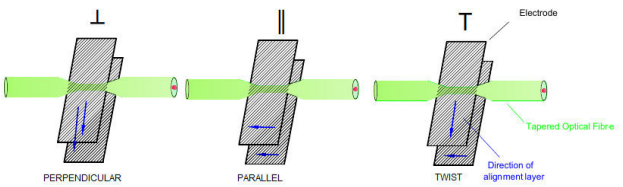

Fig. 4. Glasses layout with LC orientation layers.

The conductive layer made of ITO allowed the use of an external electric field which made it possible to change the orientation (change the director) of molecules and, as a result, change the LC RI seen by the wave propagating in the TOF structure. The spacers used were 40 µm thick and this thickness was taken as the thickness of the cell. The selection of such spacers was made during the basic research to optimize the system and cell manufacturing process. Optical adhesive NOA76 (Norland Optical Adhesive), cured under the influence of the ultraviolet radiation, was used to connect the glasses and TOF. An important technological element was the appropriate positioning of the TOF in the cell to avoid additional losses and to ensure that the taper waist area was closed in the cell. To control the correct positioning of the TOF in the cell area, a CCD camera with long focal length lenses was used (Fig. 5).

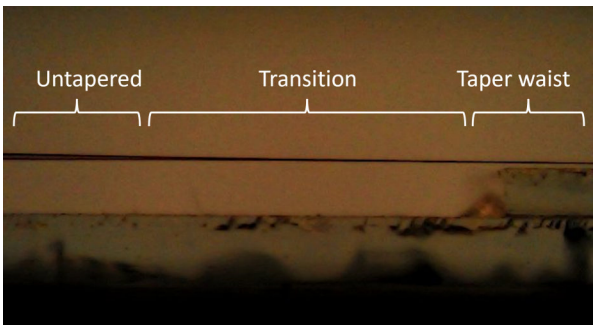

(a)

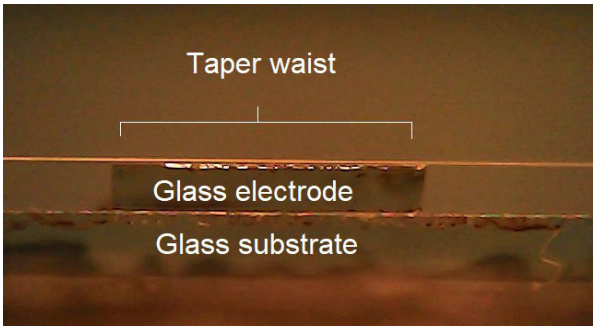

(b)

Fig. 5. Placing a TOF over a glass plate during the cell construction for LC filling.

An important part of the analysis is the LC molecules orientation around the TOF in the cell without and with Au:NPs (Fig. 6). Theoretically, the arrangement of molecules around TOF is characterized by large distortions of the director [44]. The arrangement of the molecules around the TOF reflects the surface of the fibre (Fig. 6). NPs also distort the arrangement of molecules in the cell volume. For the more dense NPs, there will be a smaller ordering parameter. It is worth recalling that in the research, the changes in the transmitted light beam through the structure in a given spectral range are the result of a change in the arrangement of the LC director under the influence of an applied voltage, which made it possible to reorient the arrangement of molecules anchored on the

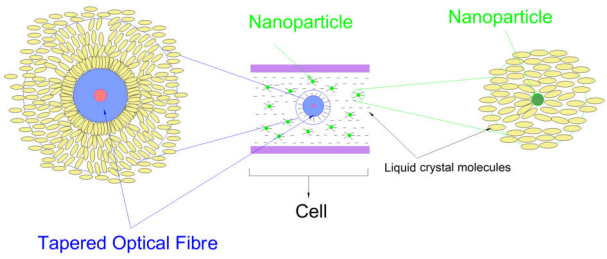

Fig. 6. Orientation of LC molecules around TOF in a cell with pure LC and LC doped with Au:NPs.

TOF surface. The anchoring energy on the surface is high, as well as the cell diameter of around 40 μm causes that in order to be able to influence the orientation of molecules around the TOF, high voltages (in the range of 20–200 V) are used during tests which allow to reorient all LC molecules around the TOF and, thus, affect changes in the parameters of the guided light. The electric field strength was in the range of 0.5–5 V/μm.

The nematic LC 1550* mixture used for the tests has well-described properties in the article, where the manufacturing process was also described [49]. The most important parameters from the point of view of the study presented in this paper are the RI and the transition temperature to the isotropic liquid. During the selection of the LC mixture, it was observed that there are few LC mixtures characterized by such low RIs – close to the RI of the optical fibre. For the LC 1550* mixture, the ordinary RI (n_o) oscillates within the RI of the optical cladding (about 1.462). After exceeding the temperature of 34 °C, n_o is characterized by a lower value than the RI TOF (< 1.459). In contrast, the extraordinary RI (n_e) of this mixture is higher than the cladding of the fibre (1.528). With increasing temperature, both RIs decrease and LC becomes isotropic liquid (> 79.8 °C) whose RI (n_i) is lower than the TOF cladding. The RI value of the used material is a very important parameter during a hybrid combination with TOF, especially regarding insertion losses and influence on the propagating wave ('evanescent wave'). Although the value of n_e is higher than the RI of the selected SMF, the light transmission was achieved through the TOF surrounded by LC. The obtained transmission is the result of correctly selected TOF geometrical parameters and may also result from the structure of the cell which consists of glass plates that limit the light and cause internal reflection of light in the structure. It should also be assumed that TOF detects the mean RI in the TOF specific region resulting from the arrangement of the LC molecules around the cylindrical fibre. The Au:NPs used for NPsLCC were obtained by the Brust-Schoffrin method [46] and were characterized by a diameter of 10 nm. The gold nanoparticles were synthesized at the Institute of Optoelectronics, Military University of Technology, Warsaw, Poland.

3. Results

Transmission measurements were carried out in the wavelength range of 500–1200 nm. The remaining wavelengths were attenuated due to the arising boundary condition, especially the difference between RIs of the taper and the surrounding material, so this range was chosen. The measurement system consisted of SuperK Extreme EXR-15 laser (NKT Photonics) operating in the wavelength range of 400–2400 nm set at 12% power, splitter (NKT Photonics) with two split ranges: NIR/IR and VIS/NIR, optical spectrum analyser AQ6373 (Yokogawa) operating in the range of 350–1200 nm, DG1022 signal generator (RIGOL), voltage amplifier A400D (FLC Electronics), and climate chamber (Votsch) [Fig. 7(a)]. The LC was controlled by a voltage with a frequency of 2 kHz – a rectangular signal and modulated by changing the waveform of the electric signal (rectangular shape) at a given frequency. The signal was in the form of AC. Voltages in the range of 0–200 V were used during the tests. Measurements of time courses were at a wavelength of 846 nm by a system containing a source of light LP852-SF30 (ThorLabs), detector PDA36A-EC (ThorLabs) operating in the range of 350–1100 nm, oscilloscope DSO-X 2012A (Agilent Technologies) [Fig. 7(b)]. The power of laser was 0.30 mW. The generator and voltage amplifier were the same.

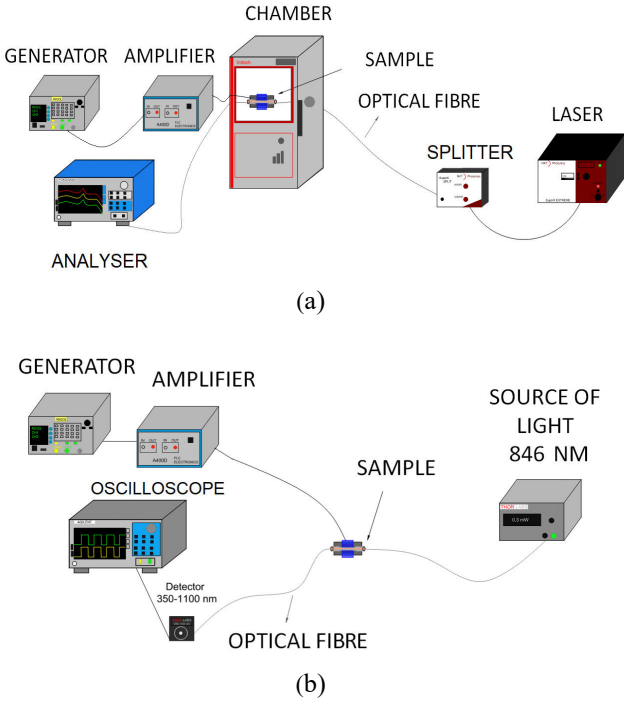

Fig. 7. Optical system set up for: transmission measurement dependent on temperature and parameters of electric signal (a) and time courses measurement (b).

Figure 8 shows the spectral characteristics for three types of orientation for the LC cell filled with a pure LC 1550* mixture at a temperature of 20 °C. Also, the transmission reference value of the TOF without the surrounding LC is marked here. After filling the cell, a decrease in power was observed for the cell with no voltage applied. This is due to the RI value of the LC mixture used which is characterized by a higher RI value than the optical fibre.

Spectral characteristics show that the light transmission is possible in the wide wavelength range of 550–1150 nm. The remaining wavelengths are effectively attenuated/absorbed by the surrounding LC TOF. For each of them, both the transmission and the range of transmitted wavelengths increase with the voltage. This is due to the change in the mean arrangement of the LC director in the cell volume, and, thus, the change in the effective RI (n_{eff}) that TOF detects. For higher voltage between 160–200 V, the average value of RI of the medium is close to the taper RI which allowed to keep the propagation properties. The maximum transmission for all orientations cells was in the 550–750 nm range and is the result of the strong entrapment of shorter wavelengths in the TOF structure, as the waves of these lengths are characterized by a lower penetration depth. Higher losses were observed for the twisted cell without the application of voltage. However, as the value of voltage increased, the effect was similar to that for the other two orientations.

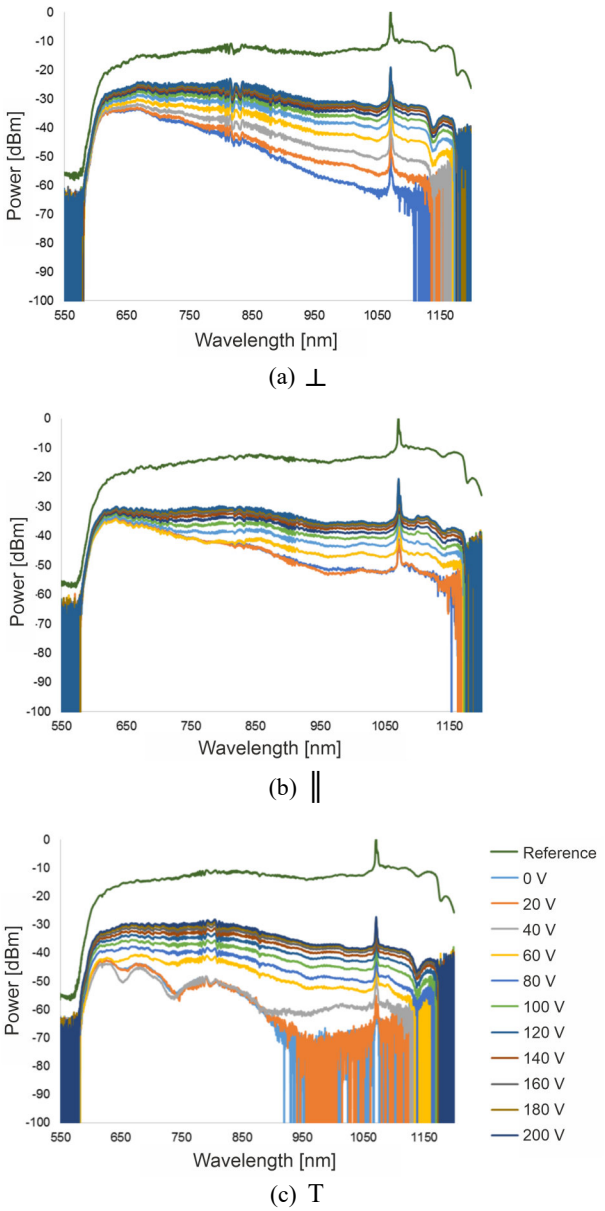

Fig. 8. Spectral characteristics at 20 °C for cell filling with a pure LC 1550* in the voltage range of 0–200 V with the orientation of layers to the fibre axis: perpendicular (a), parallel (b), and twist (c).

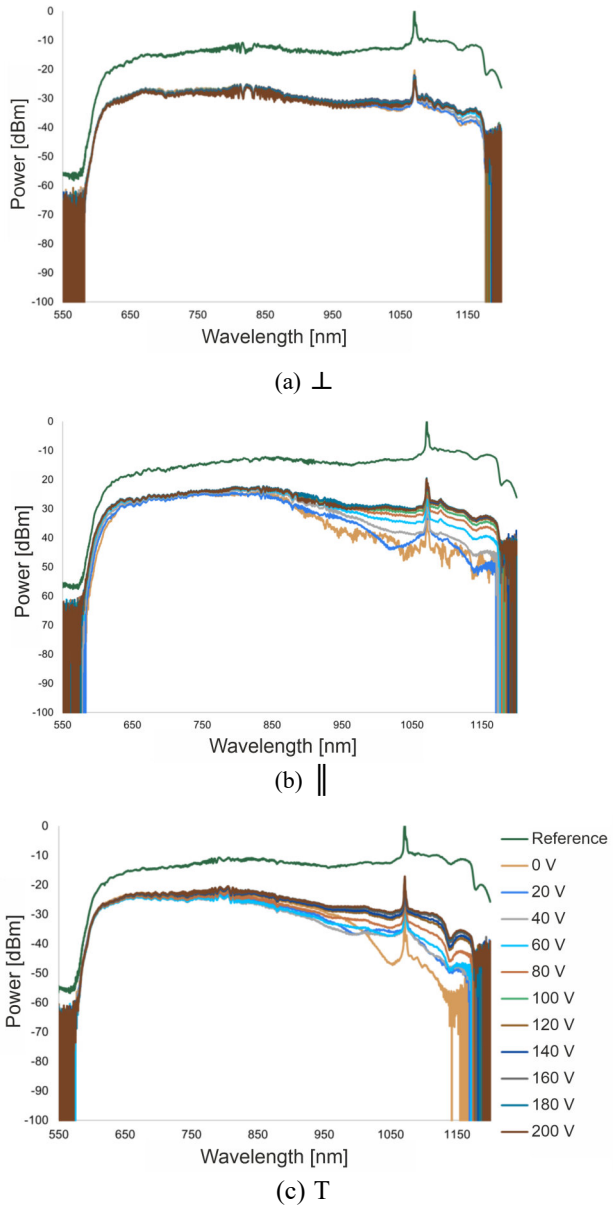

Fig. 9. Spectral characteristics at 40 °C for cell filling with a pure LC 1550* in the voltage range of 0–200 V with the orientation of layers to the fibre axis: perpendicular (a), parallel (b), and twist (c).

By increasing the temperature to 40 °C and analyzing the spectral characteristics (see Fig. 9), it can be seen that the difference between the applied voltage of 20 V and 200 V is much lower than in the case of LC at room temperature in the same voltage range. As it was mentioned earlier, it depends on decreasing the difference between RI of LC which means the change of effective RI (n_{eff}) of LC that will detect the TOF.

Taking into account the fact that for a temperature above 34 °C, n_o of LC is lower than the RI of the TOF structure, an increase in power and a smaller influence of the applied voltage on the transmission changes were observed. The comparison of power changes for the spectral characteristics for different temperatures and voltages is important because it will become a reference to the determination of the role of introducing NPs into the structure of different concentrations on the structure transmission.

Additionally, there were studies carried out on the basis of which it can be observed that the influence of the modulation of the electrical signal on the shape of spectral characteristics for each of the cells can be fully controlled (Fig. 10). It proved that the presented solution of LC and TOF can be an active optical element for which it is possible to control the attenuation and amplification of the chosen wave range depending on applied parameters of the controlling electrical signal (frequency, signal shape, applied voltage). The lower the frequency, the larger are the areas of the amplified and attenuation wavelengths. The presented transmission studies prove that TOF detects a change in the RI of the surrounding LC. Combining these two elements, with the optimal TOF geometrical parameters and correspondingly low RI LC allows controlling and tuning the light transmission. During the research, a significant role of temperature was observed which

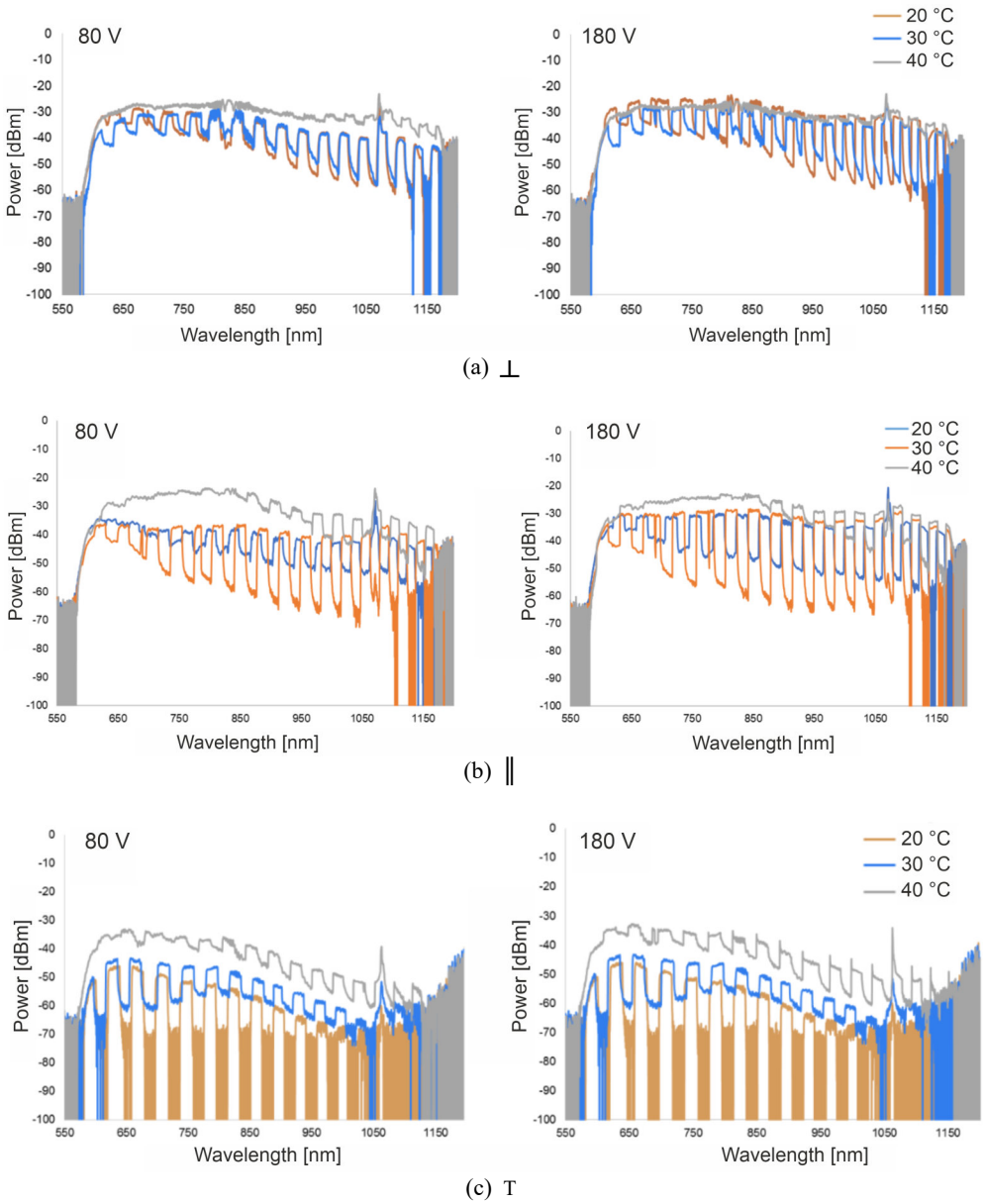

Fig. 10. Spectral characteristics at 20 °C to 40 °C for cell filling with a pure LC 1550* for applied voltages of 80 V and 180 V with additional modulation of signal (frequency of 5 Hz) for the orientation of layers to the fibre axis: perpendicular (a), parallel (b), and twist (c).

determines the RI. The modulation effect disappears (about 50 °C). When temperature rises, the difference between n_o and n_e is lower. Also, this effect is connected with the change of the structure from the nematic to isotropic state of LC. The differences between the maximum and minimum power are less noticeable for higher temperatures. TOF detects a smaller difference between the average value of n_{eff} – which is primarily responsible for losses in the structure. The more the RI LC drops below the RI TOF value (≈ 1.46), the smaller the losses are because then the ideal boundary condition, close to the initial, is obtained. Approaching the LC transition temperature to the isotropic liquid (T_{ISO} = 79.8 °C), the power of light propagated in the structure is close to the reference value of power. This effect is observed for each cell orientation.

The next part of the paper describes the results of the research whether TOF with the modified NPsLCC material will have a positive effect on the sensitivity and effectiveness of the hybrid structure. Figure 11 shows the spectral characteristics of TOF and NPsLCC, characterized by the concentration of Au:NPs 0.1 wt.% at 20 °C. Figure 12 shows the spectral characteristics of the transmission changes for the variable control field of 0–200 V at 40 °C. As it can be seen, with voltage increases there is also a visible increase of light power propagating through the structure. The maximum power is for all length of 550–750 nm which is similar to the pure LC 1550*. The highest losses for a cell with an orientation twist for 0 V can be observed.

For LC doping with 0.1 wt.% of Au:NPs at 40 °C, a reduction of influence of voltage change on the spectral characteristics was observed for all kinds of the initial orientation of molecules. Comparing the obtained spectral characteristics for both of the above temperatures, it can be seen that the voltage influence on the spectral characteristics is stronger for lower temperatures – for temperatures above 34 °C, these changes are insignificant.

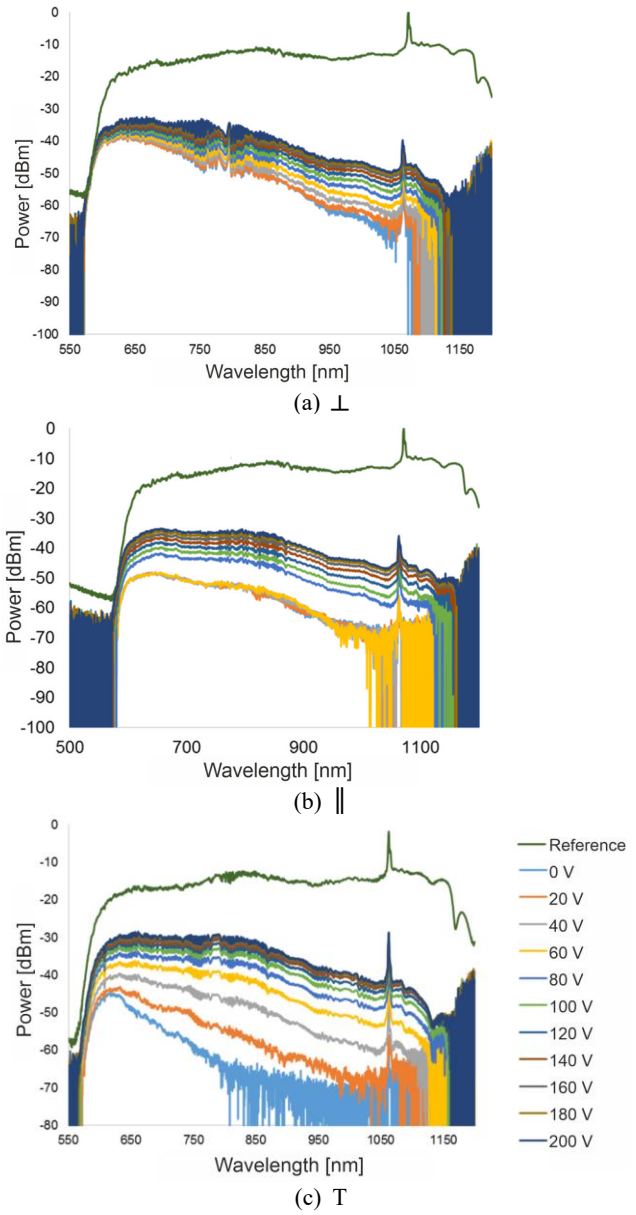

Fig. 11. Spectral characteristics at 20 °C for cell filling with an NPsLCC – concentration of Au:NPs 0.1 wt.% with the voltage range of 0–200 V with the orientation of layers to the fibre axis: perpendicular (a), parallel (b), and twist (c).

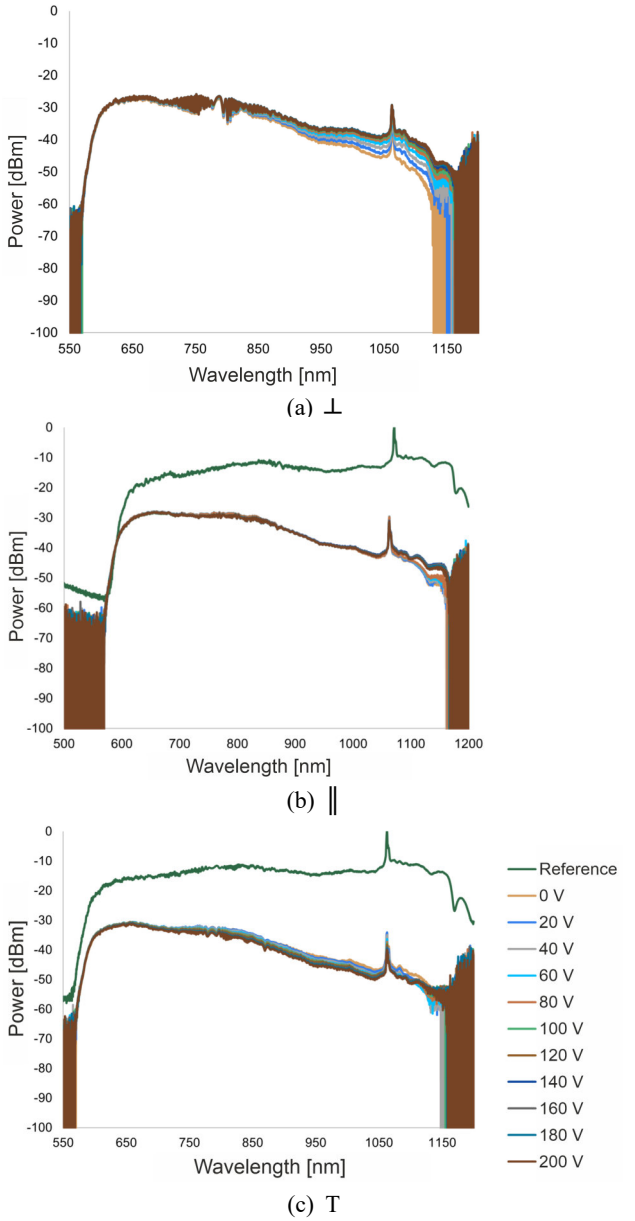

Fig. 12. Spectral characteristics at 40 °C for cell filling with an NPsLCC – concentration of Au:NPs 0.1 wt.% with the voltage range of 0–200 V with the orientation of layers to the fibre axis: perpendicular (a), parallel, and twist (c).

This behaviour is similar to that of a cell filled with a pure LC 1550* and, as described in the previous section, it is directly related to the temperature variation in RI of this mixture which is a hybrid TOF cladding. This effect is observed for all orientations.

The effect of doping 0.1 wt.% of Au:NPs into the LC on the active response of the system, i.e., transfer of rectangular modulation of different frequency and voltage for the same external parameters as in the reference measurement is shown in Fig. 13. The general behaviour of the cells is similar to that of cells with pure LC 1550*. As temperature increases, the modulation depth decreases and eventually disappears due to the decreasing RI difference of the anisotropic LC structure. For a temperature of 20 °C, the signal shape is best mapped in the whole measurement range. It is worth noting that for higher voltage, deeper changes between the maxima and the minima are visible. In the graphs, you can compare the values for 80 V and 180 V. As it can be seen compared to the pure LC 1550*, NP doping introduces higher losses in the whole range. For perpendicular orientation for 80 V and 180 V, a decrease in signal level can be observed and the modulation shape is worse than in the pure mixture. For parallel orientation, despite the decrease in power, the shape of the transmitted frequency is closer to the set frequency. The best improvement is observed for twist configuration for which the shape of frequencies is achieved for all temperatures and the differences of the modulation between minimum and maximum are higher. For this doping, NP influences the setting of the molecule director which is related to a better conductivity of the mixture which allowed a faster switching time of all mixtures. LC doping affected the change in switching times. The switching times informed how fast the TOF reacted to changes in the RI of LC. Figure 14 shows the time courses for a pure LC and NPsLCC with a concentration of 0.1 wt.%. In general, an increase in voltage results in an increase in the transmission level for all kinds of filling. As can be seen, when compared

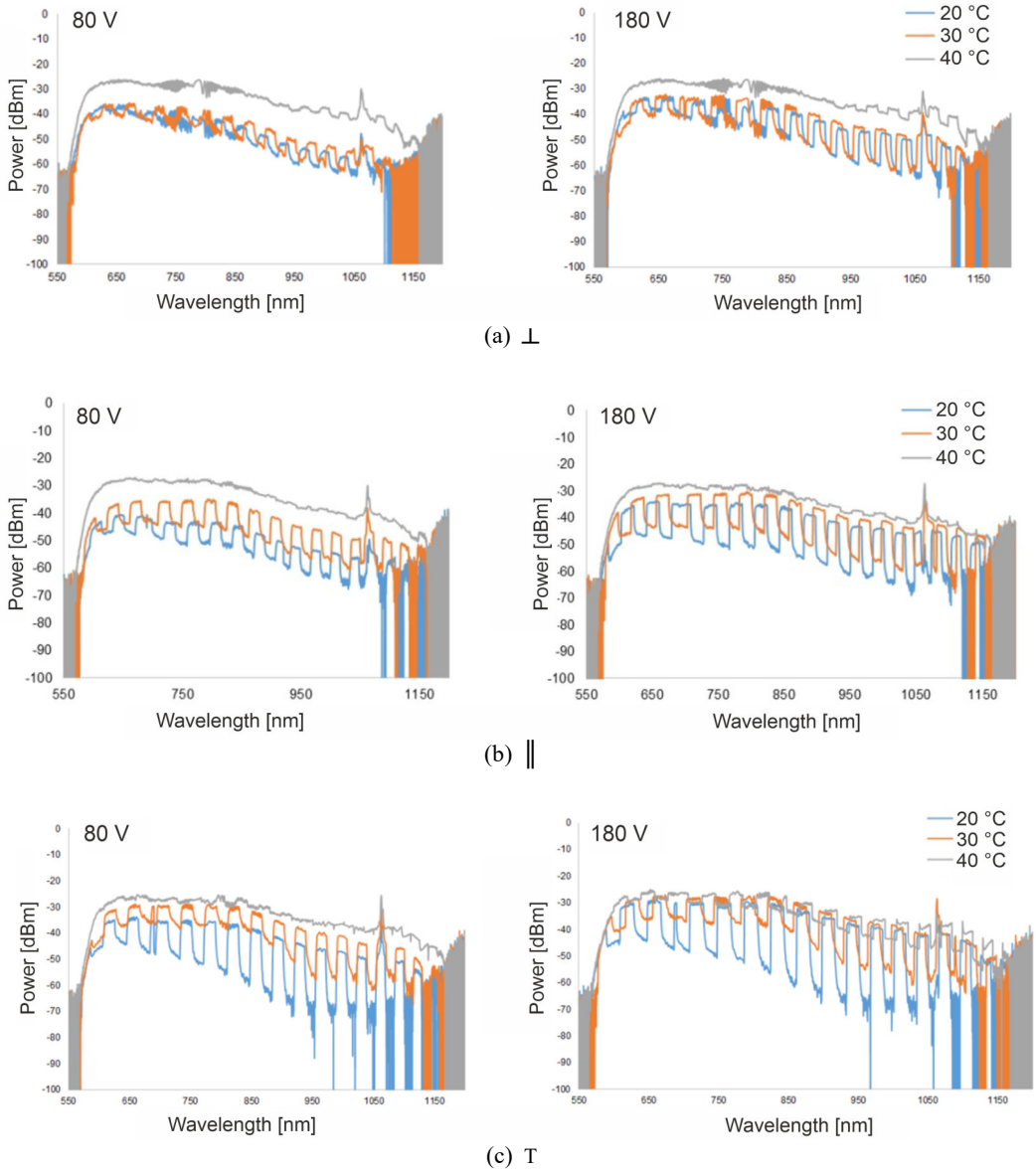

Fig. 13. Spectral characteristics at 20 °C to 40 °C for cell filled with an NPsLCC – concentration of Au:NPs 0.1 wt.% for applied voltages of 80 V and 180 V with additional signal modulation of signal (frequency of 5 Hz) for the orientation of layers to the fibre axis: perpendicular (a), parallel (b), twist (c).

to the pure LC 1550* time courses, doping with NPs causes time course changes and visible fluctuations which may be related to the vibrations that NPs and LC molecules anchored around them may experience. The switching times for cells with NPsLCC with concentrations of 0.1 wt.% were characterized by shorter ON/OFF times (Fig. 15). The time required to change the light transmission by the tested LC cell from 10% to 90% (or *vice versa*) of its maximum value with the control voltage on (or off) was assumed as the 'on' time t_{ON} (t_{OFF}).

In the next stage of the research, NPsLCC with a concentration of 0.3 wt.% of Au:NPs was used to fill the LC cell which generally resulted in an increase in losses compared to the pure LC 1550* or the NPsLCC system with 0.1 wt.%. Au:NPs. It is known that the introduction of NPs into LC causes local director distortions – hence, the more NPs added, the higher is the disturbance of the arrangement of molecules in the cell volume. Thus, it is possible to obtain the effect of 'loss of birefringence' due to large disturbances in the orientation (ordering parameter) of LC molecules in the cell. In this case, the NPs make it difficult to reorient the structure according to the external field used. As shown below, as the voltage increases, the transmission through the structure increases, but the changes in relation to the previous cells are smaller. The maximum transmission also falls in the 550–750 nm range for all three orientations. The problem encountered with this concentration is the agglomeration of NPs. This agglomeration causes strong absorption and an emerging problem with distorted directors resulting from large NPs clusters. At high dimension of NPs, LC molecules arrange themselves on the NP surface and cause further distortions of the director which directly affect the losses. To be able to influence the director changes, it is necessary to overcome the anchoring energy which results from the arrangement of LC molecules on the surface of agglomerated NPs (Fig. 16).

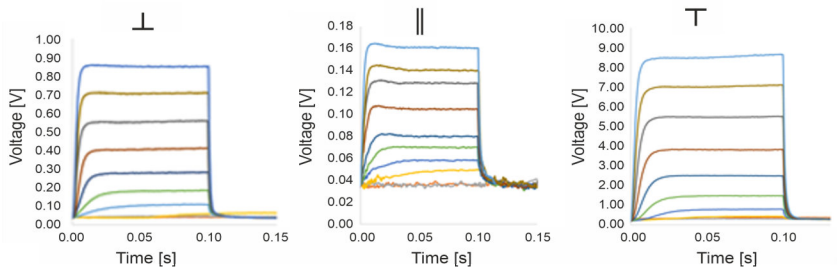

(a) Pure LC 1550

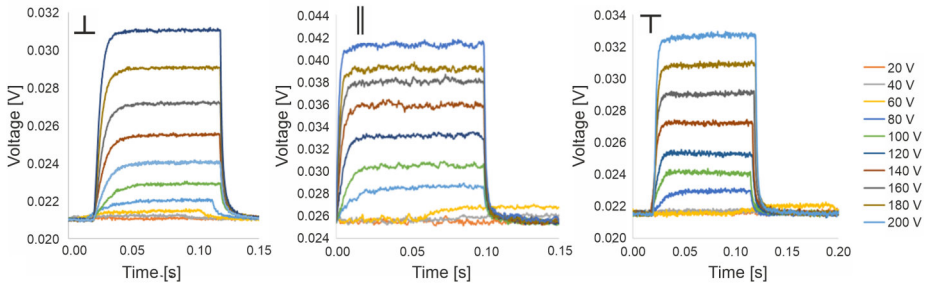

(b) NPsLCC – concentration of AuNPs 0.1 wt.%

Fig. 14. Time courses for different kinds of cell filled with pure LC (a) and NPsLCC – concentration of Au:NPs 0.1 wt.% (b). Frequency: 5 Hz, the signal shape: square, voltage range: 20–200 V, temperature: 20 °C.

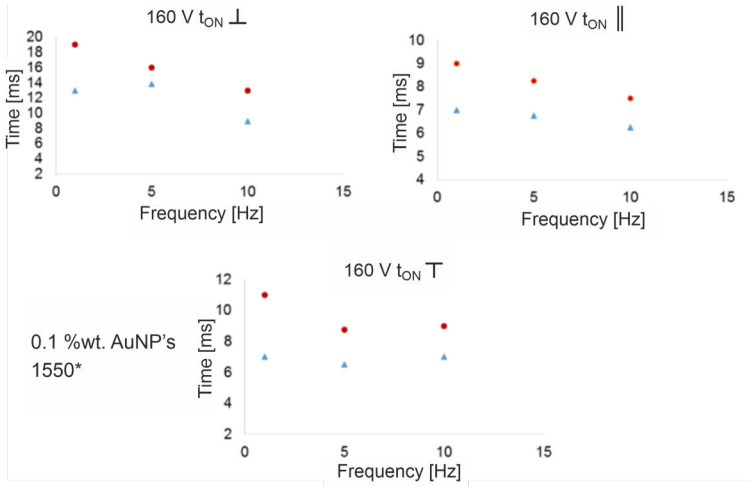

(a) t_{ON}

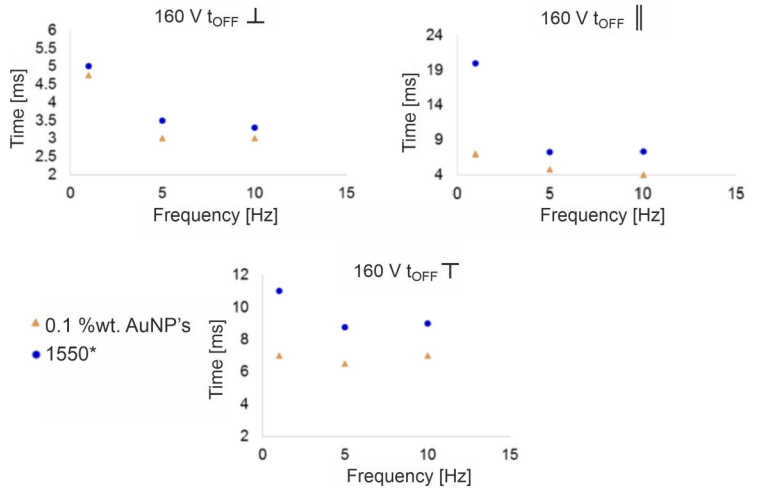

(b) t_{OFF}

Fig. 15. Times ON (a) and OFF (b) for 20 °C for pure LC and cell filling with NPsLCC – concentration of Au:NPs 0.1 wt.% with a voltage of 160 V for different frequency.

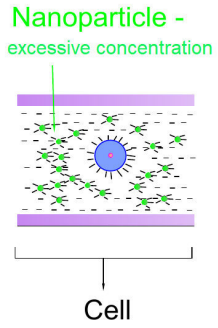

Fig. 16. LC cell with a TOF filled with NPsLCC – a high concentration of Au:NPs.

As mentioned in the introduction, the obtained spectral characteristics for a 0.3 wt.% doped mixture of Au:NPs show high power losses in relation to converters with pure LC or doping 0.1 wt.%. The increase in the transmission level with the voltage increase is slight, even for 200 V, this also applies to different temperatures (20 °C and 40 °C) – Figs. 17 and 18.

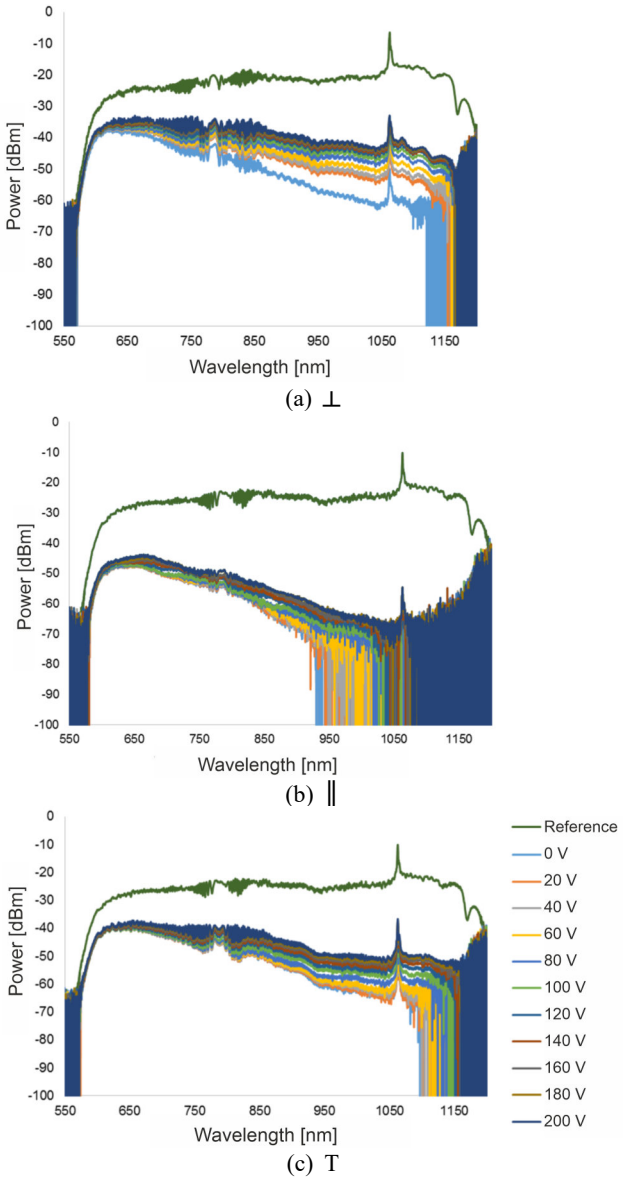

Fig. 17. Spectral characteristics at 20 °C for cell filling with NPsLCC – concentration of Au:NPs 0.3 wt.% with the voltage range of 0–200 V with the orientation of layers to the fibre axis: perpendicular (a), parallel (b), and twist (c).

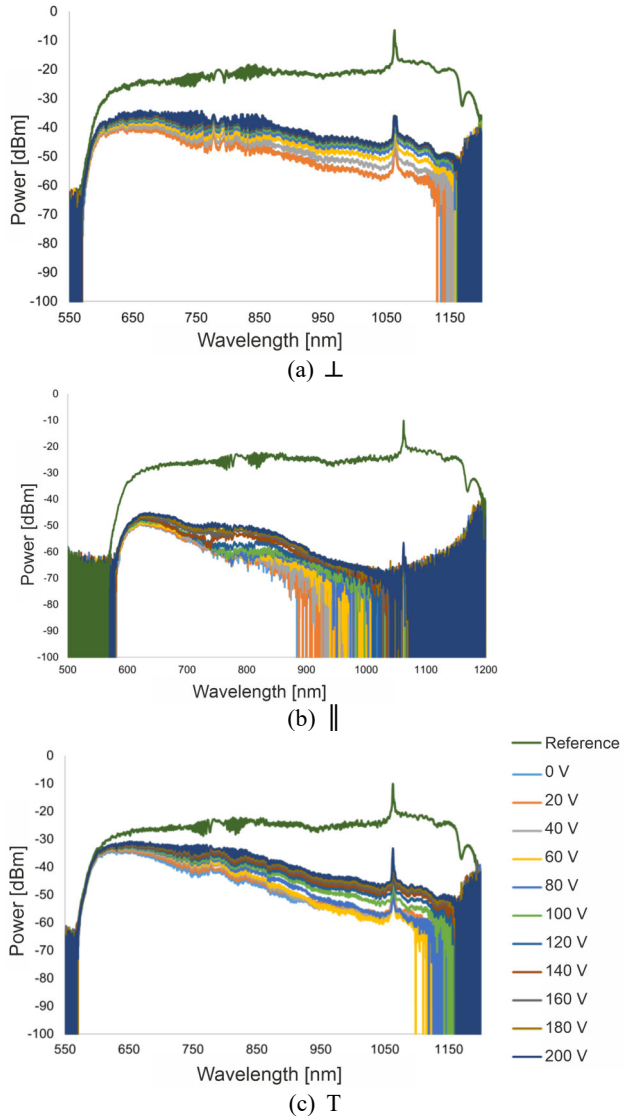

Fig. 18. Spectral characteristics at 40 °C for cell filling with NPsLCC – concentration of Au:NPs 0.3 wt.% with the voltage range of 0–200 V with the orientation of layers to the fibre axis: perpendicular (a), parallel (b), and twist (c).

Observed changes of the transmission level for a temperature of 40 °C for 0.3 wt.%. have a different character than previously for pure LC and LC doped with 0.1 wt.%. In the case of doping 0.3 wt.%. Au:NPs temperature change (from 20 °C to 40 °C) did not significantly change the transmission level even for a change of voltage.

Mapping of the modulation shape on the spectral characteristics for NPsLCC with 0.3 wt.%. is distorted, as shown in Fig. 19. The direct effect on the visible fluctuations and changes is, as mentioned above, the excessive concentration of NPs used for this transducer and the resulting disturbance of the LC molecule ordering parameter which causes agglomeration. In this case, it is also possible to ionize the parent material. Ionization can result from the addition of too many NPs which are highly conductive and increase the current density at the surface. The result is a change in the switching time of molecules, which is observed in the spectral characteristics as visible disturbances in the shape of the signal. This effect is reproduced regardless of the applied voltage for each orientation. Although the modulated signal is much worse

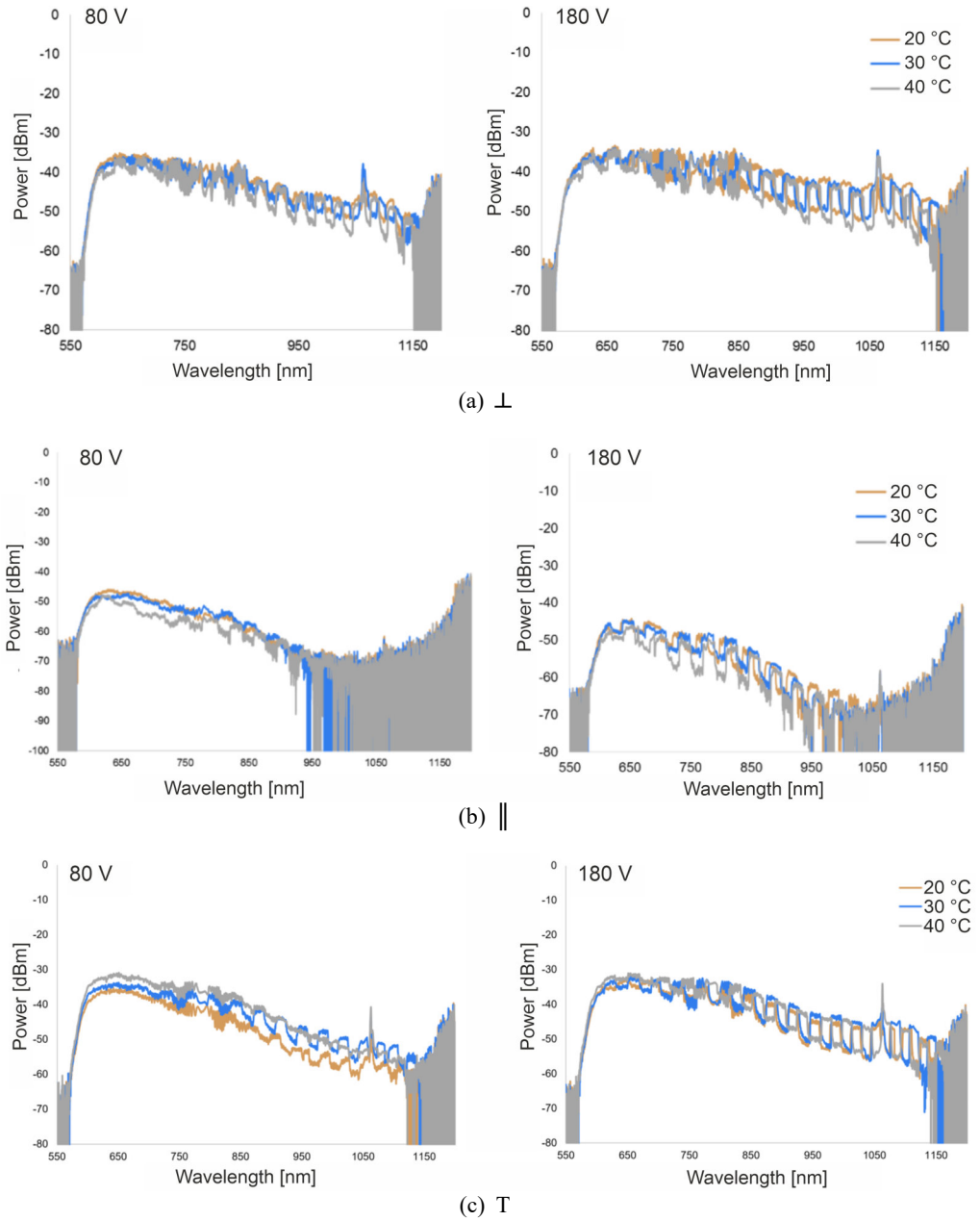

Fig. 19. Spectral characteristics at 20 °C to 40 °C for cell filling with NPsLCC – concentration of AuNPs 0.3 wt.% for applied voltages of 80 V and 180 V with additional signal modulation (frequency 5 Hz) for the orientation of layers to the fibre axis: perpendicular (a), parallel (b), and twist (c).

than for a pure mixture or doped with 0.1 wt.%, it is worth to mention that the cell with TOF still allows for light propagation. The modulation depth is almost double that of the resting measurement.

The time courses obtained for all kinds of cells were characterized by large fluctuations, as shown in Fig. 20. Measurements were made for different photodetector gains to be able to obtain results for constant laser power. For a cell with 0.3 wt.%., the Au:NPs used the highest gain because the NPs caused the high signal loss. Due to very high distortions of time courses and the possibility of making a calculation error, the switching times for these samples were not counted.

4. Discussion

Recently, many publications have shown that NPs improve the electro-optical properties of LC because they can affect LC response times and the reduction of the threshold voltage. However, as observed in the results of the measurements, the concentration of NPs in NPsLCC can strongly influence the intrinsic properties of such a doped LC. Analyzing individual cases, it should be stated that the doping of Au:NPs with a concentration of 0.1 wt.%. is the best solution for cells with the TOF. It is characterized by the best transmission and better switching times. LC doping of 0.3 wt.%. Au:NPs to TOF-based transducers causes deterioration of transmission parameters. At the same time, the use of NPs admixtures with a higher concentration introduces additional technological problems and distortion of the modulation signal shape. One of the key issues is NPs aggregation, as well as possible ionization.

In the future, the research on transducers based on TOF and NPsLCC will be continued and will allow supplementing the results already obtained and presented

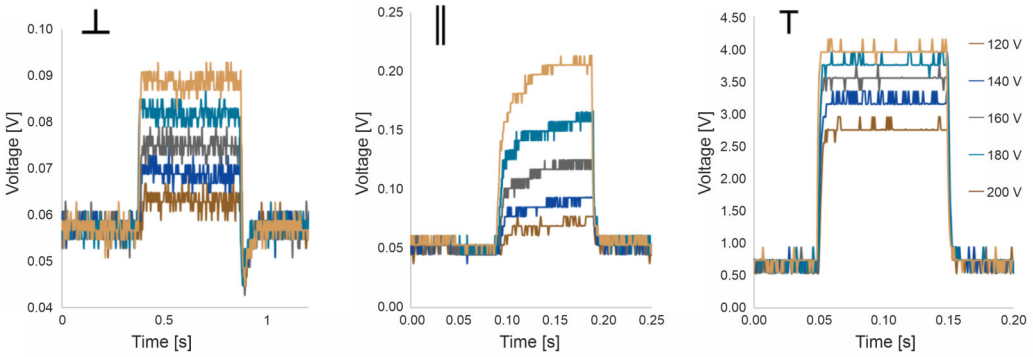

Fig. 20. Time courses for different kinds of cells filled with NPsLCC – concentration of Au:NPs 0.3 wt.% – frequency: 5 Hz, signal shape: square, voltage range: 120–200 V, temperature: 20 ˚C.

in the article. A more detailed study of the causes of the phenomena that are observed in this type of transducer is planned. It is also necessary to refine the structure of the cell, due to the fact that LCs are hygroscopic materials and are characterized by the aging process that affects their properties. Additionally, it should be noted that the absorbed OH^- ions have a destructive effect on the properties of the glass from which the fibres are made. Hence, one of the next technological elements should be the production of a cell that is hermetically closed. It is also necessary to synthesize new LC materials having an RI below the RI of the cladding, which would guarantee light transmission on the standard fibre propagation properties and allow maintenance of the boundary condition. In the future, a mixture of LC with smaller NPs could be used. It is possible that a higher concentration of smaller NPs will not aggregate and losses could be reduced. In the next step of the technological process, it will be possible to obtain a thinner cell thickness, which will directly reduce the value of the threshold voltage. An additional important element will be the application of an LC orienting layer around the TOF, which should also reduce the voltage needed to change the orientation of the director. There are many ways to apply such a layer on glass surfaces (rubbing, photopolymerization, etc.). However, the optical parameters of such a layer must be taken into account, as well as the method of its application. The layer should not significantly affect the losses and should not limit the effect on the spectral characteristics that are observed for such transducers. The method of applying the layer should also take into account the low mechanical strength of TOF. The next step is to use other LCs that can operate over a wider spectral range and to choose LCs that have shorter switching times.

Conclusions

The experimental research, presented in the article, concerns the subject of the possibility of effective control of the parameters of light guided through the TOF. The conducted research on such a hybrid combination creates the potential for the construction of many new optoelectronic devices with better parameters than the existing solutions. Taking into account the fact that many research trends related to the discipline of materials engineering are aimed at improving the parameters of existing materials, performing tests with admixture of nanoparticles show 'the path' whether a given combination allows improving the properties of a given material, which is important from the point of view of future applications and further research. The hybrid combination of TOF with NPsLCC and pure LC will find in the future direct applications as band filters, fibre optic sensors, and electro-optical switches. The article shows that the important parameters are the concentration of NPs, the geometrical parameters of TOF and RI of the selected LC.

Authors' statement

Research concept and design, J. M and K. S.; collection and/or assembly of data, J. M.; data analysis and interpretation, J. M, K. S., L. R. J. writing the article, J. M., and K. S.; critical revision of the article, L. R.J.; final approval of article, L. R. J.

Acknowledgements

This research was funded by the Ministry of Science and Higher Education as a statutory activity UGB-22-791 of the Technical Physics Applications Department of the Military University of Technology.

References

[1] Taha, B. A. *et al*. Comprehensive review tapered optical fiber configurations for sensing application: trend and challenges. *Biosensors* **11**, 253 (2021). https://doi.org/10.3390/bios11080253

[2] Joe, H.-E., Yun, H., Jo, S.-H., Jun, M. B. G. & Min, B.-K. A review on optical fiber sensors for environmental monitoring. Int. *J. Pr. Eng. Man.-Gr.* **5**, 173–191 (2018). https://doi.org/10.1007/s40684-018-0017-6

[3] Korposh, S., James, S. W., Lee, S.-W. & Tatan, R. P. Tapered optical fibre sensors: current trends and future perspectives. *Sensors* **19**, 2294 (2019). https://doi.org/10.3390/s19102294

[4] Adhikari R., Chauhan, D., Mola, G. T. & Dwivedi, R. P. A review of the current state-of-the-art in Fano resonance-based plasmonic metal-insulator-metal waveguides for sensing applications. *Opto-Electron. Rev.* **29**, 148–166 (2021). https://doi.org/10.24425/opelre.2021.139601

[5] Elosua, C. *et al*. Micro and nanostructured materials for the development of optical fibre. *Sensors* **17**, 2312 (2017). https://doi.org/10.3390/s17102312

[6] Tong, L. Micro/nanofibre optical sensors: challenges and prospects. *Sensors* **18**, 903 (2018). https://doi.org/10.3390/s18030903

[7] Moś, J., Stasiewicz, K., Matras-Postołek, K. & Jaroszewicz, L. R. Thermo-optical switching effect based on a tapered optical fiber and higher alkanes doped with ZnS:Mn. *Materials* **13**, 5044 (2020). https://doi.org/10.3390/ma13215044

[8] Wang, P., Zhao, H., Wang, X., Farrell, G. & Brambilla, G. A Review of multimode interference in tapered optical fibers and related applications. *Sensors* **18**, 858 (2018). https://doi.org/10.3390/s18030858

[9] Komaneca, M. *et al*. Structurally-modified tapered optical fiber sensors for long-term detection of liquids. *Opt. Fiber Technol.* **47**, 187–191 (2019). https://doi.org/10.1016/j.yofte.2018.11.010

[10] Ni, K., Chan, C. C., Dong, X. & Li, L. Temperature independent accelerometer using a fiber Bragg grating incorporating a biconical taper. *Opt. Fiber Technol.* **19**, 410–413 (2013). https://doi.org/10.1016/j.yofte.2013.05.008

[11] Wieduwilt, T., Bruckner, S. & Bartelt, H. High force measurement sensitivity with fiber Bragg gratings fabricated in uniform waist fiber tapers. *Meas. Sci. Technol.* **22**, 075201 (2011). https://doi.org/10.1088/0957-0233/22/7/075201

[12] Xuan, H., Jin, W. & Zhang, M. CO2 laser induced long period gratings in optical microfibers. *Opt. Express* **17**, 21882–21890 (2009). https://doi.org/10.1364/OE.17.021882

[13] Fan, P. *et al*. Higher-order diffraction of long-period microfiber gratings realized by arc discharge method. *Opt. Express* **24**, 25380–25388 (2016). https://doi.org/10.1364/OE.24.025380

[14] Tian, Z., Yam, S. S.-H. & Loock, H. P. Refractive index sensor based on an abrut taper Michelson interferometer in single mode Fiber. *Opt. Lett.* **33**, 1105–1107 (2008). https://doi.org/10.1364/OL.33.001105

[15] Bhardwaj, V., Kishor, K. & Sharma, A. C. Tapered optical fiber geometries and sensing applications based on Mach-Zehnder Interferometer: A review. *Opt. Fiber Technol.* **58**, 1–12 (2020). https://doi.org/10.1016/j.yofte.2020.102302

[16] Pu, S., Luo, L., Tang, J., Mao, L. & Zeng, X. Ultrasensitive refractive-index sensors based on a tapered fiber coupler with Sagnac loop. *IEEE Photon. Technol. Lett.* **28**, 1073–1076 (2016). https://doi.org/10.1109/LPT.2016.2529181

[17] Chen, Y., Yan, S.-C., Zheng, X., Xu, F. & Lu, Y.-G. A miniature reflective micro-force sensor based on a microfiber coupler. *Opt. Express* **3**, 24443–2450 (2014). https://doi.org/10.1364/OE.22.002443

[18] Wu, Y., Zhang, T. H., Rao, Y. J. & Gong, Y. Miniature interferometric humidity sensors based on silica/polymer microfiber knot resonators. *Sens. Actuators B Chem.* **155**, 258–263 (2011). https://doi.org/10.1016/j.snb.2010.12.030

[19] Li, X. & Ding, H. A stable evanescent field based microfiber knot resonator refractive index sensor. *IEEE Photon. Technol. Lett.* **26**, 1625–1628 (2014). https://doi.org/10.1109/LPT.2014.2329321

[20] Lach C. N. H. C., Jamaludin, N., Rokhani, F. Z., Rashid, S. A. & Noor, A. S. M. Lard detection using a tapered optical fiber sensor integrated with gold-graphene quantum dots. *Sens. Bio-Sens. Res.* **26**, 100306 (2019). https://doi.org/10.1016/j.sbsr.2019.100306

[21] Korec, J., Stasiewicz, K. A., Garbat, K. & Jaroszewicz, L. R. Enhancement of the SPR Effect in an optical fiber device utilizing a thin ag layer and a 3092A liquid crystal mixture. *Molecules* **26**, 7553 (2021). https://doi.org/10.3390/molecules26247553

[22] Lin, H.-Y., Huang, Ch.-H., Cheng, G.-L., Chen, N.-K. & Chui, H.-Ch. Tapered optical fiber sensor based on localized surface plasmon resonance *Opt. Express* **20**, 21693–21701 (2012). https://doi.org/10.1364/OE.20.021693

[23] Socorro, A. B., Del Villar, I., Corres, J. M., Arregui, F. J. & Matias I. R. Spectral width reduction in lossy mode resonance-based sensors by means of tapered optical fibre structures. *Sens. Actuators B Chem.* **200**, 53–60 (2014). https://doi.org/10.1016/j.snb.2014.04.017

[24] Stasiewicz, K. A., Jakubowska, I. & Dudek, M. Detection of organosulfur and organophosphorus compounds using a hexafluorobutyl acrylate-coated tapered optical fibers. *Polymers* **14**, 612 (2022). https://doi.org/10.3390/polym14030612

[25] Zhu, S. *et al*. High sensitivity refractometer based on TiO_2-coated adiabatic tapered optical fiber via ALD technology. *Sensors* **16**, 1295 (2016). https://doi.org/10.3390/s16081295

[26] Wang, S., Feng, M., Wu, S., Wang, Q. & Zhang, L. Highly sensitive temperature sensor based on gain competition mechanism using graphene coated microfiber. *IEEE Photon. J.* **10**, 6802008 (2018). https://doi.org/10.1109/JPHOT.2018.2827073

[27] Zubiate, P., Zamarreño, C. R., Del Villar, I., Matias, I. R. & Arregui, F. J. Graphene enhanced evanescent field in microfiber multimode interferometer for highly sensitive gas sensing. *Opt. Express* **22**, 28154–28162 (2014). https://doi.org/10.1364/OE.22.028154

[28] Korec, J., Stasiewicz, K. A., Strzeżysz, O., Kula, P. & Jaroszewicz, L. R. Electro-steering tapered fiber-optic device with liquid crystal cladding. *J. Sensors* **2019**, 1–11 (2019). https://doi.org/10.1155/2019/1617685

[29] Moś, J. *et al*. Research on optical properties of tapered optical fibers with liquid crystal cladding doped with gold nanoparticles. *Crystals* **9**, 306 (2019). https://doi.org/10.3390/cryst9060306

[30] Marć, P., Stasiewicz, K., Korec, K., Jaroszewicz, L. R & Kula, P. Polarization properties of nematic liquid crystal cell with tapered optical fiber *Opto-Electron. Rev.* **27**, 321–328 (2019). https://doi.org/10.1016/j.opelre.2019.10.001

[31] Talataisong, W., Ismaeel, R. & Brambilla, G. A review of microfiber-based temperature sensors. *Sensors* **18**, 461 (2018). https://doi.org/10.3390/s18020461

[32] Wu, X. & Tong, L. Optical microfibers and nanofibers. *Nanophotonics* **2**, 407–428 (2018). https://doi.org/10.1515/nanoph-2013-0033

[33] Vishnoi, G., Goel, T. & Pillai, P. K. C. Spectrophotometric studies of chemical species using tapered core multimode optical fiber. *Sens. Actuators B Chem*. **45**, 43–48 (1997). https://doi.org/10.1016/S0925-4005(97)00268-2

[34] Zhang, L., Lou, J. & Tong, L. Micro/nanofiber optical sensors. *Photonic. Sens.* **1**, 31–42 (2011). https://doi.org/10.1007/s13320-010-0022-z

[35] Wiejata, P., Shankar, P. & Mutharasan, R. Fluorescent sensing using biconical tapers. *Sens. Actuators B Chem.* **96**, 315–320 (2003). https://doi.org/10.1016/S0925-4005(03)00548-3

[36] Moayyed, H., Teixeira Leite, I., Coelho, L., Santos, J. & Viegas, D. Analysis of phase interrogated SPR fiber optic sensors with biometallic layers. *IEEE Sens. J.* **14**, 3662–3668 (2014). https://doi.org/10.1109/JSEN.2014.2329918

[37] Zubiate, P., Zamarreño, C. R., Del Villar, I., Matias, I R. & Arregui, F. J. High sensitive refractometers based on lossy mode resonance supported by ITO coated D-shape optical fibers. *Opt. Express* **23**, 8045–8050 (2015). https://doi.org/10.1364/OE.23.008045

[38] Budaszewki, D. *et al*. Nanoparticles-enhanced photonic liquid crystal fibers. *J. Mol. Liq*. **267**, 271–278 (2018). https://doi.org/10.1016/j.molliq.2017.12.080

[39] Tian, Y., Wang, W., Wu, N., Zou, X. & Wang, X. Tapered optical fiber sensor for label-free detection of biomolecules. *Sensors* **11**, 3780–3790 (2011). https://doi.org/10.3390/s110403780

[40] Brambilla, G. *et al.* Optical fiber nanowires and microwires: fabrication and applications. *Adv. Opt. Photonics* **1**, 107–161 (2009). https://doi.org/10.1364/AOP.1.000107

[41] Prakash, J., Khan, S., Chauhan, S. & Biradar, A. M. Metal oxide-nanoparticles, and liquid crystal composites: A review of recent progress. *J. Mol. Liq.* **297**, 112052 (2020). https://doi.org/10.1016/j.molliq.2019.112052

[42] Khatua, S. *et al*. Plasmonic nanoparticles−liquid crystal composites. *J. Phys. Chem. C* **114**, 7251–7257 (2010). https://doi.org/10.1021/jp907923v

[43] Podoliak, N. *et al*. Elastic constants, viscosity and response time in nematic liquid crystals doped with ferroelectric nanoparticles. *RSC Adv.* **4**, 46068–46074 (2014). https://doi.org/10.1039/C4RA06248E

[44] Choudhary, A., Singh, G. & Biradar, A. M. Advances in gold nanoparticle–liquid crystal composites. *Nanoscale* **6**, 7743–7756 (2014). https://doi.org/10.1039/C4NR01325E

[45] Przybysz, N., Marć, P., Tomaszewska, E., Grobelny, J. & Jaroszewicz, L. R. Mixtures of selected n-alkanes and Au nanoparticels for optical fiber threshold temperature transducers. *Opto-Electron. Rev.* **28**, 220–228 (2021). https://doi.org/10.24425/opelre.2020.136111

[46] Budaszewski, D. *et al.* Enhanced efficiency of electric field tunability in photonic liquid crystal fibers doped with gold nanoparticles. *Opt. Express* **27**, 14260–14269 (2018). https://doi.org/10.1364/OE.27.014260

[47] Qi, H. & Hegmann T. Multiple alignment modes for nematic liquid crystals doped with alkylthiol-capped gold nanoparticles. *ACS Appl. Mater. Interfaces* **1**, 1731–1738 (2009). https://doi.org/10.1021/am9002815

[48] Stamatoiu, O., Mirzaei, J., Feng, X. & Hegmann, T. Nanoparticles in Liquid Crystals and Liquid Crystalline Nanoparticles. in *Liquid Crystals. Topics in Current Chemistry* (ed. Tschierske, C.) **318,** 331–393 (Springer, Verlag Berlin Heidelberg 2012). https://doi.org/10.1007/128_2011_233

[49] Dąbrowski, R. *et al.* Low-birefringence liquid crystal mixtures for photonic liquid crystal fibres application. *Liq. Cryst.* **44**, 1911–1928 (2017). https://doi.org/10.1080/02678292.2017.1360952